Atmospheric Environment 201 (2019) 101–109

Contents lists available at ScienceDirect

Atmospheric Environment

journal homepage: www.elsevier.com/locate/atmosenv

Important role of aromatic hydrocarbons in SOA formation from unburned gasoline vapor

Tianzeng Chen[a,c], Yongchun Liu[a,c,d,*], Changgeng Liu[a], Jun Liu[a,c], Biwu Chu[a,b,c], Hong He[a,b,c,**]

[a] State Key Joint Laboratory of Environment Simulation and Pollution Control, Research Center for Eco-Environmental Sciences, Chinese Academy of Sciences, Beijing, 100085, China

[b] Center for Excellence in Regional Atmospheric Environment, Institute of Urban Environment, Chinese Academy of Sciences, Xiamen, 361021, China

[c] University of Chinese Academy of Sciences, Beijing, 100049, China

[d] Beijing Advanced Innovation center for Soft Matter Science and Engineering, Beijing University of Chemical Technology, Beijing, 100029, China

GRAPHICAL ABSTRACT

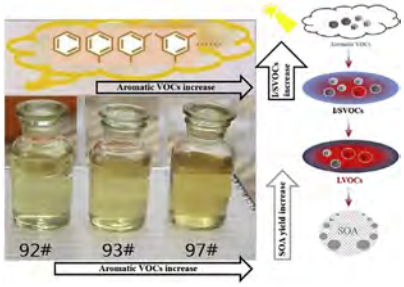

ARTICLE INFO

Keywords:
Secondary organic aerosol
Gasoline vapor
Aromatic content
Semi-volatile organic compounds

ABSTRACT

Gasoline emissions are the largest source of urban atmospheric VOCs, which are critical precursors of ozone (O_3) and secondary organic aerosol (SOA). Besides vehicle exhaust, emissions from gasoline evaporation also have a potentially significant effect on SOA formation. However, there are still few studies on the relationship between gasoline vapor composition and SOA formation, especially for gasoline in China. In this study, SOA formation from three unburned gasoline vapors were investigated in a 30 m^3 indoor smog chamber. The experimental results showed that with the increase of aromatic content (especially toluene and C2 benzenes) in gasoline from 23% to 50%, the SOA yield was significantly enhanced by a factor of 4.0–6.7. This phenomenon might be related to the higher amounts of intermediate volatility organic compounds (IVOCs) and semi-volatile organic compounds (SVOCs) formed, which promoted the gas-particle partitioning and SOA formation. Additionally, the synergistic effects between precursors in the mixtures might also be a key factor, which could be supported by the higher SOA yield accompanied by a higher ratio of toluene/benzene. Meanwhile, there were more oxygenated organic aerosols (OOA) observed when using high-aromatic gasoline. This work will help in understanding the effect of aromatic content or gasoline quality on the SOA formation from gasoline evaporation emissions, and in providing the scientific basis for taking corresponding control measures to relieve haze events in China.

* Corresponding author. State Key Joint Laboratory of Environment Simulation and Pollution Control, Research Center for Eco-Environmental Sciences, Chinese Academy of Sciences, Beijing, 100085, China.

** Corresponding author. State Key Joint Laboratory of Environment Simulation and Pollution Control, Research Center for Eco-Environmental Sciences, Chinese Academy of Sciences, Beijing, 100085, China.

E-mail addresses: liuyc@buct.edu.cn (Y. Liu), honghe@rcees.ac.cn (H. He).

https://doi.org/10.1016/j.atmosenv.2019.01.001
Received 20 July 2018; Received in revised form 15 November 2018; Accepted 2 January 2019
Available online 04 January 2019

1. Introduction

Volatile organic compounds (VOCs) play a crucial role in regional air quality since they are important precursors of O_3 and secondary organic aerosol (SOA) (Huang et al., 2014; Liu et al., 2010), which are associated with human health risks, climate change and visibility reduction (Davidson et al., 2005; Pöschl, 2005; Thalman et al., 2017). Previous studies have shown that vehicular emissions were the largest source of urban atmospheric VOCs. For example, vehicular emissions contributed about 36–48% of VOCs in Beijing in 2014, 25% in Shanghai from 2007 to 2010, 30–53% in the Pearl River Delta (PRD) in 2004, respectively (Cai et al., 2010; Liu et al., 2008; Wu et al., 2016). As the most widely used vehicle fuel, gasoline has a huge transportation energy consumption rate around the world, such as in China and the USA (EIA, 2018; NBSC, 2017). Smog chamber experiments have extensively proved that VOC precursors in gasoline exhaust could significantly contribute to the SOA formation via the photo-oxidation processes occurring under different experimental conditions (Gentner et al., 2012; Gordon et al., 2014; Liu et al., 2015b; Nordin et al., 2013; Platt et al., 2014; Zervas et al., 1999; Zhao et al., 2017). Moreover, results derived from field observations also suggested that gasoline exhaust plays a dominate role in SOA formation and that SOA concentrations would be significantly reduced with a decrease in gasoline emissions on local and global scales (Bahreini et al., 2012).

Vehicular emissions not only include the exhaust emitted from the tailpipes of gasoline-powered vehicles, but also include the emissions released from evaporation of gasoline (e.g. headspace emissions, refueling, etc.) and liquid gasoline (e.g. leakage, hot soak, spillage, and running loss, etc.) (Choi and Ehrman, 2004; Song et al., 2007; Watson et al., 2001). It has been found that the contribution of evaporative emissions to the total VOC emissions was up to 12% in Beijing, 4.6% in Japan, ranked as the 6th-highest source, and even more than 30% for other developed countries (Song et al., 2007; Van der Westhuisen et al., 2004; Yamada, 2013). And with the implementation of tailpipe exhaust emission control measures, the proportion of evaporation loss (unburned gasoline in particular) has shown an increasing trend (Liu et al., 2015a). Meanwhile, evaporative emission inventory studies indicate that vehicular evaporative emissions have become an increasingly important source of VOCs in China, with up to 124,000 tons released from refueling processes in 2010 (Yang et al., 2015). Therefore, more attention should be paid to this primary emissions source, and especially its associated secondary formation of particulate matter (PM).

Aromatic hydrocarbons are a class of unsaturated chemical substances with at least one benzene ring, and they play a crucial role and account for approximately 30% of gasoline fuels (Gentner et al., 2013). Odum et al. (1997) have indicated that SOA formation from the photo-oxidation of gasoline vapor almost completely depended on the aromatic hydrocarbons in it (Odum et al., 1997). Meanwhile, different influences of unburned fuel composition (e.g. carbon number and molecular structure) on SOA formation potential have been investigated, finding that with the increase of carbon-number and/or aromatic hydrocarbon contents in the unburned fuels, more SOA were formed generally. As for the gasoline-related SOA formation, it was more sensitive to the content of aromatic hydrocarbons (Jathar et al., 2013). Similarly, previous studies have also shown that with the high content of aromatics in gasoline fuel, more primary PM as well as aromatic VOCs will be released in the gasoline exhaust (Karavalakis et al., 2015; Wang et al., 2016; Zervas et al., 1999). In addition, Peng et al. (2017) have expounded on the relationship between SOA production and gasoline exhaust composition as affected by the variable aromatic content in different fuels (quality level: China phase V). They reported that with the gasoline aromatic content elevated from 29% to 37%, there was a marked enhancement of SOA production (up to 3–6 times) (Peng et al., 2017). It should be noted that the quality of gasoline, such as the content of sulfur and aromatic hydrocarbons, varied greatly among different provinces (Karavalakis et al., 2015; Tang et al., 2015). However, there have been few reports on SOA formation directly from gasoline vapor or on the links between SOA potential and the aromatic content, especially for gasoline in China.

In this study, experiments on SOA formation from the photo-oxidation of unburned gasoline vapors were performed in a 30 m^3 indoor smog chamber. We utilized three different gasoline fuels obtained from different gas stations (e.g., from Hebei and Beijing), in the presence of NO_x, at levels comparable to ambient conditions, to investigate the relationship between the SOA formation potential and the corresponding gasoline vapor composition, especially regarding aromatics. Finally, according to the results derived from this study, we also proposed science-based suggestions to reduce the contribution of evaporation emissions from gasoline-related usage processes to ambient SOA.

2. Materials and methods

2.1. Fuels

In this study, three gasoline samples (G1, G2 and G3) collected (with the standard Method for manual sampling of petroleum liquids (GB/T 4756-2015) as a guideline) from different gas stations, were utilized to examine the effects of gasoline vapors on SOA formation. They were all commercial phase China V gasoline with equivalent octane numbers of 97 (G1), 93 (G2), and 92 (G3), respectively. Their characteristics are shown in Table 1, and the details of the compositions are given in Table S1. G1 gasoline contained the highest aromatic content (50.5%) among the samples, followed by G2 gasoline (39.6%), and the aromatic content was the lowest (22.8%) for G3 gasoline. The higher aromatic content in G1 is due to some VOCs (e.g., aldehydes, ketones, alcohols ethers, and methyl *tert*-butyl ether (MTBE)) not being taken into account. These VOCs are undetectable by GC-MS due to the lack of standards or the separation capacity of the GC column. However, these species are unlikely to be SOA precursors in our experiments because of their low molecular weight (carbon number ≤ 6) and in the absence of seed particles (Kroll et al., 2005; Zhao et al., 2017). These gasoline samples were similar in olefin content and are commercially available on the Chinese market, such as in Beijing and Hebei.

2.2. Experimental simulation

Experiments on SOA formation from gasoline vapors were carried out in a 30 m^3 indoor smog chamber at the Research Center for Eco-Environment Sciences, Chinese Academy of Sciences (RCEES-CAS). Fig. S1 shows the schematic structure of the smog chamber (see Supplementary Material). Briefly, the chamber is a cuboid reactor (4.0 m (height) × 2.5 m (width) × 3.0 m (length)) with a surface-to-volume ratio of 1.97 m^{-1}, lined with 125 μm-thick FEP100 film (DuPont™, US). The chamber reactor is located in a temperature-controlled room, in which the temperature (T) and relative humidity (RH) can be controlled mechanically. In order to ensure sufficient mixing of the gas-phase species, a three-wing stainless steel fan coated with Teflon was installed at the bottom inside the reactor.

Meanwhile, the chamber was equipped with a series of gas- and particle-phase monitoring instruments. NO_x and O_3 were measured using a chemiluminescence NO_x analyzer (Model 42i-TL, Thermo Fisher

Table 1
Parameters of the gasoline utilized in this study.

Specifications	G1	G2	G3
Octane number	97	93	92
Aromatics (% v/v)	50.5	39.6	22.8
Olefin (% v/v)	7.9	7.3	12.1
Quality level	China phase V	China phase V	China phase V

Scientific) and a UV photometric O_3 analyzer (Model 49i, Thermo Fisher Scientific), respectively. VOCs contained in gasoline were monitored with a gas chromatograph (7890B GC, Agilent, USA) equipped with a DB-624 column (60 m × 0.25 mm × 1.40 μm, Agilent, USA) and a mass spectrometry detector (5977A MS, Agilent, USA). In addition, gas-phase hydrocarbons and their intermediate products were also measured with a high-resolution time-of-flight proton transfer reaction mass spectrometer (HR-ToF-PTRMS) (Ionicon Analytik GmbH). The particle size distribution and number concentration were measured using a scanning mobility particle sizer (SMPS, TSI, USA), which was composed of a differential mobility analyzer (DMA, 3080 Classifier, TSI, USA) coupled with a condensation particle counter (CPC, 3776, TSI, USA). The mass concentration was calculated based on the volume concentration with the typical SOA density of 1.4 g cm^{-3} (Ng et al., 2007). Moreover, the mass concentration and chemical composition of SOA were measured using a high-resolution time-of-flight aerosol mass spectrometer (HR-ToF-AMS, Aerodyne Research Inc. USA). Due to wall loss of particles and gaseous species on the Teflon film, the measured aerosol concentration was corrected using the method mentioned in Takekawa et al. (2003), and the gas concentrations were also corrected after considering the loss rates of them (i.e., wall loss rates of NO_2, NO, O_3 and VOCs were $(1.67 \pm 0.25) \times 10^{-4}$, $(1.32 \pm 0.32) \times 10^{-4}$, $(3.32 \pm 0.21) \times 10^{-4}$ and $(2.20 \pm 0.39) \times 10^{-4}$ min^{-1}, respectively), which were derived from the additional separate experiments. Finally, temperature (T) and relative humidity (RH) were monitored real-time using a hydro-thermometer (Vaisala HMP110).

Prior to each experiment, the Teflon chamber was cleaned by purified and dry zero air for about 24 h at a flow rate of 100 L min^{-1} until almost no NO_x could be detected or the particle number concentration was < 10 cm^{-3}. Before the experiments, a known volume of liquid gasoline was carried by purified dry zero air through a heated Teflon line system into the chamber. NO was subsequently carried by purified dry zero air into the chamber. The concentrations were continuously monitored at a measurement point in the reactor until they were stable, ensuring that the components in the reactor were well mixed. The experiment was then conducted for about 6 h with the UV lights on and the fan turned off. All the experiments were carried out at a temperature of 25 ± 2 °C and dry conditions (RH < 10.0%). The detailed experimental conditions are listed in Table S2.

3. Results

3.1. Simulation of SOA formation from different unburned gasoline vapors

Fig. 1 shows the time-resolved concentrations of gas- and particle-phase species during a typical chamber experiment. In this experiment, the initial VOCs/NO_x ratio (ppbC/ppb) was 7.5, which was in the range of 5.5–15 observed in the heavy haze events in China (An et al., 2016; Zou et al., 2015). Moreover, within the first 20 min after the UV lights were turned on, almost all of NO was rapidly converted to NO_2. At the same time, O_3 was gradually formed and its maximum concentration was up to 350 ppb (Fig. 1a).

For the degradation of typical aromatic hydrocarbons such as benzene and toluene (Fig. 1b), which were measured by HR-ToF-PTRMS with a time resolution of 5 min, there were different decay rates due to the different reaction rates with OH radicals (Atkinson and Arey, 2003). According to the evolution of the concentration ratios for benzene and toluene, the OH exposure could be obtained to characterize the aerosol formation from the photo-oxidation of gasoline vapors (de Gouw et al., 2005). Meanwhile, the equivalent photo-oxidation aging times for the experiments were also calculated under the assumption that the OH concentration in the ambient air was 1.6×10^6 molecule cm^{-3} (Hu et al., 2013; Peng et al., 2016).

In addition, we also applied positive matrix factor (PMF) analysis to the HR-ToF-PTRMS data to separate the signals of gasoline vapor components and the multi-generation products (Liu et al., 2014; Paatero, 1997; Paatero and Tapper, 1994; Ulbrich et al., 2009). The high resolution time series of VOCs concentrations determined by HR-ToF-PTRMS were used as the inputs of the PMF analysis. The details of PMF analysis and quality assurance have been described elsewhere (Liu et al., 2014; Yan et al., 2016) and are given in the Supplementary Material. We observed the obvious consumption of other components (mainly alkenes and aromatic hydrocarbons) in the gasoline vapors during the entire photochemical reaction, such as C_4H_8 (m/z = 56), C_5H_{10} (m/z = 70), $C_6H_4(CH_3)_2$ (m/z = 106), $C_6H_3(CH_3)_3$ or $C_6H_4CH_3C_2H_5$ (m/z = 120), and $C_6H_4(C_2H_5)_2$ (m/z = 134), as shown in Fig. 2a and b (in green). This is consistent with a previous study that indicated high alkene and aromatic hydrocarbon contents in the gasoline samples collected from the cities of northern China (Tang et al., 2015). At the same time, the primary generation products, mainly composed of aldehydes and ketones, were generated (seen in Fig. 2a and c, in blue), such as $(CH_3)_2CO$ or CH_3CH_2CHO or CHOCHO (m/z = 58), C_3H_7CHO or CH_3COCHO (m/z = 72), C_4H_9CHO (m/z = 86), C_5H_9CHO or $HCO(CH)_2CH_2CHO$ or $CH_3CO(CH)_2CHO$ (m/z = 98), $C_5H_{11}CHO$ (m/z = 100), C_6H_5CHO (m/z = 106), and $CH_3C_6H_4CHO$ (m/z = 120). The contribution of these products rapidly grew until they reached the maximum point, and then gradually decreased later. Many researchers have also identified glyoxal (CHOCHO, m/z = 58), methylglyoxal (CH_3COCHO, m/z = 72), and benzaldehyde (C_6H_5CHO, m/z = 106) as the major primary ring-opening and ring-retaining products from the OH-reaction of aromatic compounds, with various yields (Atkinson et al., 1989; Baltaretu et al., 2009; Forstner et al., 1997; Gery et al., 1985; Ji et al., 2017; Klotz et al., 1998; Seuwen and Warneck, 1996; Smith et al., 1998; Volkamer et al., 2001; Wu et al., 2014). Moreover, as the reaction time went on, the contribution of the multi-generation products gradually increased (Fig. 2a, d and e, in purple and

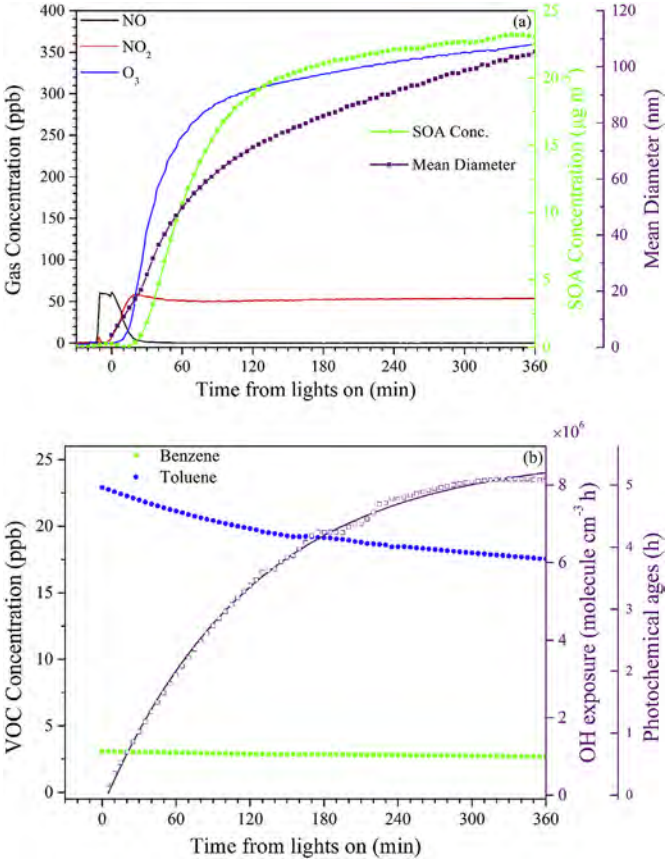

Fig. 1. Time series of NO, NO_2, O_3, particle diameter and corrected SOA (a), typical VOCs and OH exposure (b) during a typical chamber experiment (experiment G2-05).

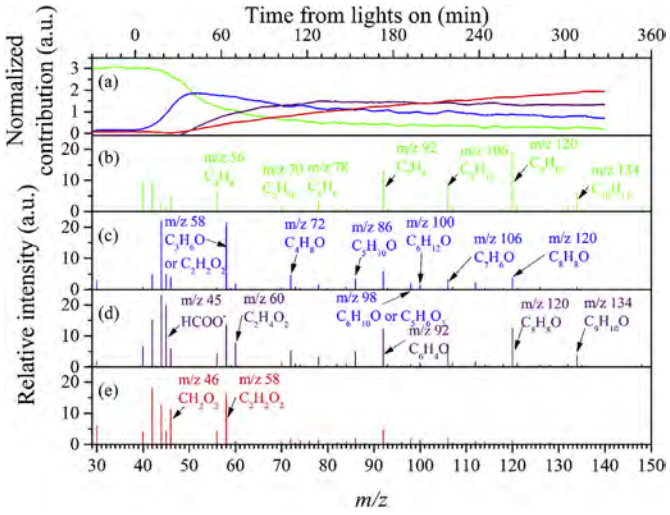

Fig. 2. Evolution of gasoline vapors compositions and the multi-generation products during the entire photochemical reaction (a); Mass spectra of typical compositions in gasoline vapor, mainly alkenes and aromatic hydrocarbons (in green) (b); Mass spectra of primary generation products (in blue) (c), secondary generation products (in purple) (d), and tertiary generation products (in red) (e). (For interpretation of the references to color in this figure legend, the reader is referred to the Web version of this article.)

red), and their main components were aldehydes and acids (such as HCOOH, CH_3COOH, etc.), which were the products accompanying the formation of low-volatility organic compounds (LVOCs) during the ring-opening process (Forstner et al., 1997). These LVOCs had low enough volatility to result in the formation of SOA through gas-particle partitioning (Kroll and Seinfeld, 2008) and make a positive contribution to new particulate formation (NPF) (Kulmala, 2003; Kulmala et al., 2004; Wang et al., 2017). It worth noting that the intensities of *m/z* 92 and *m/z* 120 in Fig. 2d were stronger than that in Fig. 2c, which might be contributed from the oxygenated products and were tentatively assigned to C_6H_4O (benzene oxide/oxepin) and C_8H_8O (tolualdehyde), respectively (Jenkin et al., 2003; Obermeyer et al., 2009; Volkamer et al., 2002). Meanwhile, according to the gas-phase chemical degradation processes of a series of VOCs described by the Master Chemical Mechanism (MCM), these aldehydes and acids were accompanied by the formation of high-molecular-weight multifunctional species (Bloss et al., 2005a, 2005b; Jenkin et al., 2003), which also contribute to the formation of SOA (Hallquist et al., 2009).

Therefore, the phenomenon of new particle formation was observed after the UV lights were turned on, and the particle number concentration reached a maximum level within 1 h (Fig. 1a). With the accumulation of secondary species on the newly formed particles, the particle diameter gradually grew from 20 to 110 nm, large enough to act as cloud condensation nuclei (CCN) (Lambe et al., 2011), which have an adverse effect on radiative forcing. Meanwhile, as can be seen from the compositions of aerosol particles derived from the HR-ToF-AMS, SOA was the main component (Fig. S2) and played a significant role in secondary particle formation from the photo-oxidation of gasoline vapors, and was similar to the composition of secondary aerosols formed from gasoline exhausts (Peng et al., 2017). Considering that the experiments in this study were conducted under dry conditions (RH < 10%) and in the absence of seed particles, the contribution of aqueous-phase and heterogeneous reactions to SOA formation could be neglected (Zhang et al., 2015a, b). Therefore, the SOA formation occurred mainly through the condensation of multi-generation products oxidized via photochemical reactions of precursors (Jathar et al., 2014; Jimenez et al., 2009; Robinson et al., 2007).

In addition, the NO^+/NO_2^+ ratio obtained by HR-ToF-AMS, often used as a proxy for identification of ammonium and organic nitrates,

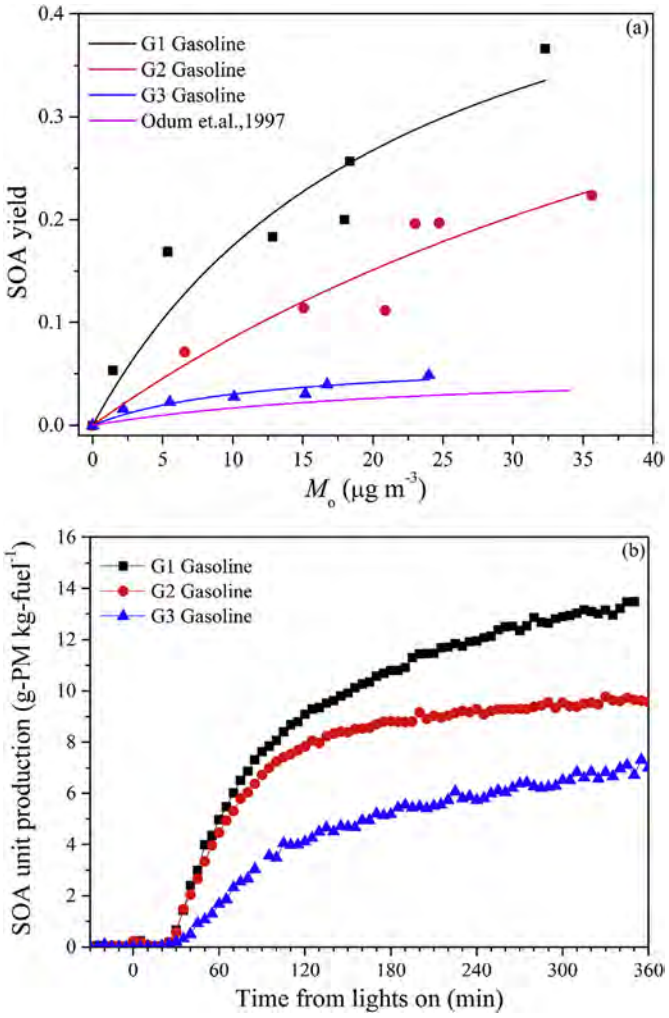

Fig. 3. SOA yields derived from photochemical oxidation of gasoline vapors as a function of SOA mass concentration (M_o) measured at 25 ± 2 °C and RH < 10% (a), unit production of SOA in typical gasoline vapor experiments (experiments G1-06, G2-05, and G3-05) as a function of photochemical oxidation time (b).

and organic nitrates, generally was higher than the NO^+/NO_2^+ ratio of ammonium nitrate (Farmer et al., 2010; Rollins et al., 2009; Sato et al., 2010). In this study, the NO^+/NO_2^+ ratios for all experiments were 6.27–6.87, which were obviously higher than the ratios for ammonium nitrate (1.08–2.81) and close to those for organic nitrates (3.82–5.84) derived from the photo-oxidation of aromatic hydrocarbons (Farmer et al., 2010; Sato et al., 2010). Therefore, organic nitrates dominated the formation of nitrate and played an important role in SOA (Chu et al., 2016).

3.2. Impacts of fuel composition on SOA yield

SOA yields derived from different gasoline vapors are shown in Fig. 3. Table S2 shows the experimental conditions, including the initial concentration of VOCs, NO_x, temperature (T), and relative humidity (RH), etc. A semi-empirical model based on the gas-particle partitioning of products is widely used to describe the relationship between SOA yield and aerosol mass concentration (M_o) (Odum et al., 1996), which can be described by the following equation (1):

$$Y = \sum_i M_o \frac{\alpha_i K_{om,i}}{1 + K_{om,i} M_o} \quad (1)$$

where α_i and $K_{om,i}$ (m^3 μg^{-1}) are the mass-based gas-phase

stoichiometric fraction and gas-particle partitioning coefficient, respectively. Y is the SOA yield, and M_o is the formed aerosol mass concentration.

In this study, a one-product model was employed to fit the experimental data and could accurately reproduce the data ($R^2 = 0.91$), while models with two or more products could not significantly improve the fitting quality. The fitting parameters α determined by minimizing the sum of the squares of the residuals showed a decreasing trend as the aromatic content decreased ($\alpha = 0.62$, 0.55, and 0.07 for G1, G2, and G3, respectively). This phenomenon indicated that decreasing the aromatic content would be unfavorable for the formation of lower-volatility products, and then reduce the SOA yield (Li et al., 2016a). This is consistent with the understanding that aromatic hydrocarbons are more easily oxidized to LVOCs than long-chain alkane.

As shown in Fig. 3a, the SOA yields were positively correlated with the aromatic content in gasoline vapors. Higher aromatic content led to significant enhancement of the SOA yields. According to the SOA yield curve derived from the one-product model (Zhou et al., 2011), the SOA yield acquired at the higher aromatic content (G1 gasoline, 50.5% v/v and G2 gasoline, 39.6% v/v) was about 6.7 and 4.0 times of that for the lower aromatic content (G3 gasoline, 22.8% v/v), respectively, assuming that the mass loading was 25 $\mu g\, m^{-3}$, which was the average PM_1 mass concentration observed during a typical pollution process at a regional receptor site (Peng et al., 2016). Recent studies (Krechmer et al., 2016; Saleh et al., 2013; Trump et al., 2014; Ye et al., 2016; Zhang et al., 2014, 2015a, b) have revealed that wall losses of IVOCs and SVOCs were prone to a low bias in the effective SOA yield, which is caused by the competition between uptake of organic vapors by suspended particles and the chamber wall. This competition could be evaluated by the timescales associated with gas-to-particle partitioning ($\tau_{g\text{-}p}$) and vapor-wall loss ($\tau_{g\text{-}w}$) (Zhang et al., 2014). The underestimation of SOA yield could be approximately quantified by the ratio of them (i.e., $\tau_{g\text{-}p}/\tau_{g\text{-}w}$). According to the methods described by Zhang et al. (2014) (shown in Supplementary material), $\tau_{g\text{-}w}$ was estimated to be in the range of 58–100 min assuming an upper bound and a lower bound of molecular mass of organic vapors (MW) (100–300 $g\, mol^{-1}$). Correspondingly, $\tau_{g\text{-}p}$ were comparable among all of these experiments. For example, it was 105–182 min for G1 gasoline vapor, 108–187 min for G2 gasoline vapor and 120–209 min for G3 gasoline vapor. Therefore, the SOA yield was underestimated by a factor of 1.82–2.09 for all experiments due to the wall losses of IVOCs and SVOCs. Therefore, the enhancement of SOA yields for different gasoline experiments were not due to the biases caused by organic vapor wall losses.

From the perspective of aromatic species (i.e., benzene, toluene, C2 benzenes and C3 benzenes), the fractions of all aromatic species (except for C3 benzenes) went up in a linear way with the SOA yields from different gasoline (Fig. S3), which further indicated that the important contribution of aromatic content to SOA yield. In addition, the SOA yield curves derived from our study were higher than that in Odum et al. (1997) (Fig. 3a), to some extent, indicating the lower quality of gasoline in China compared with that in the USA (Tang et al., 2015).

Moreover, a similar enhancement role for the unit production of SOA (i.e., normalized to the amount of gasoline) with the increase of aromatic content was observed. As revealed in Fig. 3b, the maximum value for SOA unit production (13.5 g-PM $kg\text{-}fuel^{-1}$) was acquired from the gasoline vapors with highest aromatic content (G1 gasoline, 50.5% v/v), followed by G2 gasoline (39.6% v/v aromatic content) and G3 gasoline (22.8% v/v aromatic content). Meanwhile, for other experiments with the same volume of introduced gasoline (e.g., 20 μL in G1-02, G2-01, G3-01, and 60 μL in G1-04, G2-03, G3-03), the enhancement role of aromatic for the unit production of SOA was also observed (Fig. S4). Previous studies have indicated that the fuel composition, especially the aromatic content in gasoline, had a significant impact on SOA production and primary particulate emissions from exhaust experiments (Karavalakis et al., 2015; Odum et al., 1997; Peng et al., 2017; Wang et al., 2016; Zervas et al., 1999). For example, Odum et al. (1997) found that SOA production from high-aromatic-content fuels (32–48% v/v) was significantly higher (up to 3-fold) than that from low-aromatic-content fuels (20–25.5% v/v), and suggested that aromatic content played a crucial role in SOA formation from photo-oxidation of gasoline vapor (Odum et al., 1997). Previous studies have indicated that there was a synergistic effect between precursors in mixtures (i.e., anthropogenic and biogenic) (Ahlberg et al., 2017; Hildebrandt et al., 2011). Hildebrandt et al. (2011) found that under the coexistence of biogenic and anthropogenic precursors (e.g., myrcene and m-xylene, respectively), nucleation particles would readily form, and then lead to generation of more particulate mass. Meanwhile, Ahlberg et al. (2017) utilized isotope-labeled toluene and unlabeled α-pinene to generate mixtures of SOA, and discovered that the presence of anthropogenic SOA could promote the formation of biogenic SOA. Therefore, the higher SOA production accompanying higher aromatic content in gasoline vapors might be due to the synergistic effects of these aromatic hydrocarbons. Moreover, vehicle and engine experiments using different fuels conducted by Peng et al. (2017) showed that the SOA production factors derived from fuel with higher aromatic content (36.7% v/v) was 3 times that obtained using fuel with lower aromatic content (28.5% v/v) (Peng et al., 2017).

We also found that a significant proportion (63.6–80.8%) of the SOA was generated within the first 2 h during the photo-oxidation reactions (as shown in Fig. S5). This phenomenon indicated that the homogeneous nucleation process, through gas-particle partitioning, contributed a great proportion to the SOA formation (Odum et al., 1996; Pankow, 1994), which was consistent with the inherent change trend of primary and secondary generation products (which are largely intermediate volatility organic compounds (IVOCs) and semi-volatile organic compounds (SVOCs)) observed in Fig. 2c and d. Recent studies have also proved that IVOCs and SVOCs were an important source of SOA (Kroll et al., 2007; Robinson et al., 2007; Zhao et al., 2014, 2015, 2016). It could be speculated that there would be more IVOCs and SVOCs partitioned into the particle phase for the G1 gasoline experiments with the enhancement of aromatic hydrocarbon and SOA concentrations.

In addition, SOA production from photo-oxidation of VOC precursors in the gasoline vapors could be predicted by the following equation (2) (Donahue et al., 2006):

$$\Delta SOA_{predicted} = \sum_i \Delta HC_i \times Y_i \quad (2)$$

where ΔHC_i and Y_i are the degradation mass concentration of each VOC precursor i and its corresponding SOA yield, respectively. Considering the smaller contribution (~4%) of alkenes and alkanes to SOA formation (Peng et al., 2017), the selected VOC precursors were mainly benzene, toluene, C2 benzenes (i.e., o, m, p-xylene, and ethylbenzene), and C3 benzenes (i.e., trimethylbenzene, ethyltoluene, and propylbenzene) (Gordon et al., 2014; Liu et al., 2015b; Platt et al., 2013). In order to obtain a relatively believable production prediction, the yield parameters for these precursors were selected according to the $VOCs/NO_x$ ratio (Table S2), and the detailed parameters seen in Table S3.

As revealed in Fig. 4, the fraction of estimated SOA concentration ranged from 40% to 55% at the end of three typical smog chamber experiments. The largest contributions to SOA formation were from C3 benzenes, except for the experiment using G1 gasoline (experiment G1-06), which was consistent with the different percentage compositions in gasoline (Table S1). Previous studies have also indicated that the C3 benzenes (i.e., C9 aromatics) contributed significantly to SOA formation from gasoline vehicle exhaust (Gordon et al., 2014; Nordin et al., 2013; Peng et al., 2017; Platt et al., 2013). Additionally, it is worth noting that with the increase of aromatic hydrocarbon contents, the percentage of SOA formation explained by single-ring aromatic VOCs showed a decreasing trend (for G3 this was ~55%, G2 was ~50%, and G1 was ~40%). This suggested that the SOA yield based on a single

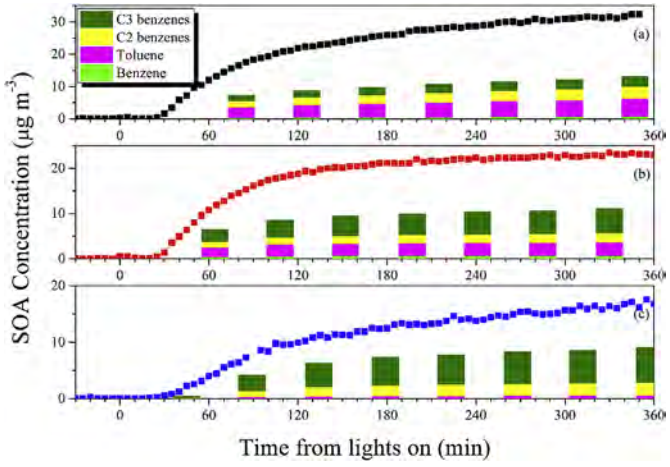

Fig. 4. Measured and estimated SOA concentration as a function of reaction time in typical smog chamber experiments (a) G1-06, (b) G2-05, and (c) G3-05. The lines and squares (colored black, red, and blue, respectively) represent the corrected SOA concentrations in the corresponding chamber experiments. The green, magenta, yellow, and olive areas represent the estimated SOA from the photo-oxidation of benzene, toluene, C2 benzenes, and C3 benzenes, respectively. (For interpretation of the references to color in this figure legend, the reader is referred to the Web version of this article.)

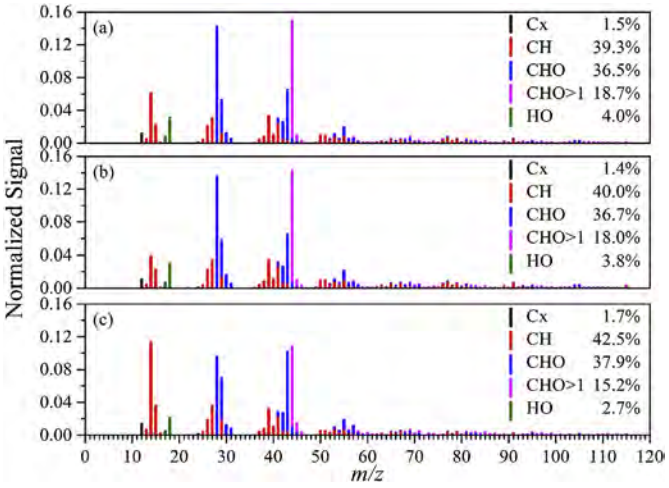

Fig. 5. Normalized mass spectra of the SOA compositions at the end of each typical smog chamber experiment (a) G1-06, (b) G2-05, and (c) G3-05. The detected ion fragments have been grouped into five families (i.e. Cx, CH, CHO, CHO > 1, and HO), therein Cx contains only carbon; CH contains only carbon and hydrogen; CHO contains carbon, hydrogen and one oxygen, CHO > 1 contains carbon, hydrogen and great than one oxygen, and HO contains only oxygen and hydrogen.

VOC precursor might be underestimated due to the synergistic effects in mixtures of precursors (Ahlberg et al., 2017; Hildebrandt et al., 2011). This synergistic effect probably exist when considering the change in the relative distribution of different aromatic species among gasoline samples. In our study, the higher SOA yield was accompanied by the higher ratio of toluene and benzene (T/B) (for G1 this value was 13.0, G2 and G3 were about 8.0) and ratio of C2 benzenes/benzene (C2−B/B) (for G1 was 10.3, G2 and G3 were 5.6). Therefore, considering the synergistic effects between these precursors (benzene, toluene, C2 benzenes, and C3 benzenes), which all have a larger proportion in G1 compared to the gasoline G2 and G3 (seen in Table S1), the estimated SOA concentration fraction was lowest for G1. Apparently, the detailed synergistic effect between different anthropogenic precursors (e.g., benzene, toluene and C2 benzenes) need to be further investigated through more experimental studies. In addition, Odum et al. (1997) have concluded that the total SOA production generated from the photo-oxidation of gasoline vapor could mostly be determined by the aromatic hydrocarbons of the fuels (the ratio of predicted SOA to actual SOA was 71–131% with an average of 100 ± 16%) (Odum et al., 1997). This might be due to the fact that some heavy aromatics (e.g., C4-benzenes, p-diethylbenzene) might present in the sample but not be detected in our study, which have substantial SOA formation potentials and thus would greatly contribute to the SOA formed from gasoline vapors. Therefore, in order to accurately predict the SOA formation, more related VOC precursors need to be detected.

3.3. Impacts of fuel composition on SOA composition

AMS data have been widely used to characterize the composition of non-refractory organic aerosols (Chen et al., 2015; Chhabra et al., 2011; Heald et al., 2010; Ng et al., 2010). The detected ion fragments have been divided into five groups according to their carbon, hydrogen and oxygen content (Nordin et al., 2013). As shown in Fig. 5, the prominent *m/z* peaks in the SOA formation from gasoline vapors are *m/z* 44 and *m/z* 43, and an analogous phenomenon was found in the SOA derived from gasoline exhaust (Nordin et al., 2013; Platt et al., 2013). Meanwhile, the *m/z* 43 and 44 signals were mainly composed of $C_2H_3O^+$ and CO_2^+ ions, respectively, for all gasoline vapor experiments (Fig. S6). These two ions both represent the oxygenated organic aerosol (OOA), and CO_2^+ in particular is a main indicator of low-volatility OOA (LV-OOA) which are generated from the decarboxylation of organic acids (Ng et al., 2010). As demonstrated in Fig. 5, the fraction of CO_2^+ showed an increasing trend (G3 15.2%, G2 18.0%, and G1 18.7%) with the elevation of aromatic content in gasoline. Correspondingly, the contribution fraction of elemental oxygen also showed an increasing trend (G3 28.5%, G2 31.8%, and G1 32.6%) with the increase of aromatic content in gasoline (Fig. S6). Considering that the aromatic hydrocarbons are more reactive with OH radicals (Atkinson and Arey, 2003), our results illustrated that with increasing content of aromatics, the gasoline vapor could be more prone to oxidize to form more LV-OOA species, which have low enough volatility to favor gas-particle partitioning into the particle phase, and thus be favorable to SOA formation (Tröstl et al., 2016).

In addition, the O:C ratio can also be used to characterize the oxidation state of organic aerosols (Chhabra et al., 2011). A van Krevelen diagram showing the H:C and O:C ratios is illustrated in Fig. 6. As shown in Fig. 6, the SOA derived from G1 gasoline vapor (highest

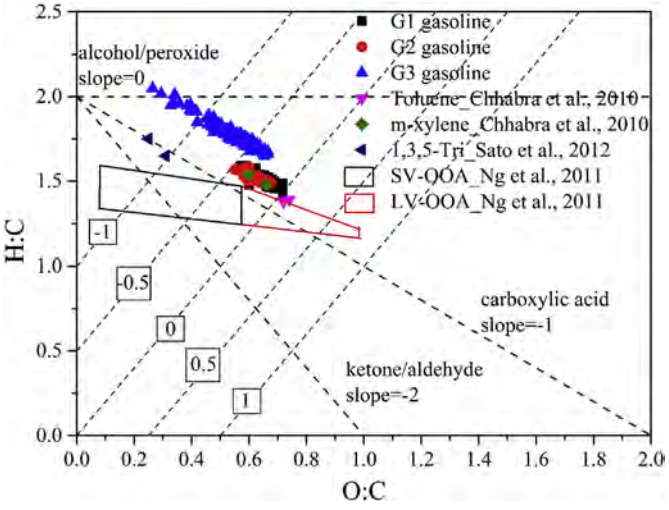

Fig. 6. Van Krevelen diagram of SOA from unburned gasoline vapors. The numbers labeling the dotted lines show the carbon oxidation state (OSc = 2×O:C - H:C). The O:C and H:C data are obtained from the end of the typical smog chamber experiments (experiments G1-06, G2-05, and G3-05).

aromatic content, 50.5% v/v) had higher O:C (0.66 ± 0.03) and carbon oxidation state (OSc = 2×O:C−H:C, −0.18 ± 0.03) compared to the SOA from G3 gasoline vapor, with the lowest aromatic content (22.8% v/v) (O:C = 0.54 ± 0.07, OSc = −0.67 ± 0.07). This was consistent with the observation that SOA generated from photooxidation of G1 vapor had a higher fraction of LV-OOA, as mentioned above (Fig. 5). Meanwhile, the value of the O:C ratio for SOA formed from G1 and G2 was close to that from toluene and m-xylene (Chhabra et al., 2010), which was consistent with the content of major aromatic compounds in G1 and G2 (seen in Table S1). However, the value of the O:C ratio for SOA generated from G3 was more similar to that from 1,3,5-trimethylbenzene (Sato et al., 2012), which was related to the relatively high abundance of C3 benzenes in G3 (seen in Table S1). This general trend of decreasing O:C and increasing H:C was also observed in previous studies, which were focused on the role of methyl group number on SOA formation from monocyclic aromatic hydrocarbons (Li et al., 2016a, 2016b). Previous studies have reported that the semi-volatile OOA (SV-OOA) and low-volatility OOA (LV-OOA) typically have O:C ratios of 0.3–0.6 and 0.6–1.0, respectively (Jimenez et al., 2009). Therefore, our results indicated that the SOA formed from G3 with lower aromatic content should be SV-OOA compounds, while SOA generated from G1 with higher aromatic content should be related to LV-OOA compounds, respectively.

4. Conclusions and implication

Our experimental results indicated that the aromatics in gasoline vapor played a significant role in SOA formation. The SOA yield was greatly enhanced (by a factor of 4.0–6.7) when high-aromatic-content gasoline was employed. The possible reason was that higher aromatic content could lead to more IVOC and SVOC formation, which could significantly partition into the particle phase and then greatly contribute to SOA yield. Apart from that, the synergistic effects between VOC precursors might also be an important reason. Meanwhile, the SOA composition derived from AMS showed that more oxygenated organic aerosols (OOA) were formed and the oxidation state (OSc) was higher when using high-aromatic gasoline.

Recently, China had implemented more stringent gasoline restriction standards, especially on gasoline sulfur content, to meet the new standard. In contrast, the aromatic content in gasoline has showed an increasing trend. For instance, a previous study reported that the average aromatic contents in commercial gasoline meeting the III, IV and V standards in Beijing were 23.4, 28.5 and 36.3%, respectively (Peng et al., 2017). Meanwhile, a recent study showed that the aromatic content of gasoline in North China (41.6%) was 9.6% higher than that in the USA (32.0%) (Tang et al., 2015). Additionally, there have been a large quantity of vehicular VOC evaporative emissions due to refueling and diurnal processes (124,000 ton in 2010) in China (Yang et al., 2015). Therefore, more attention should be paid to the quality of gasoline (especially aromatics), considering its enhancement of SOA formation derived from our study. Our findings provided a new perspective on controlling air pollution caused by vehicles. One measure that could be taken is the implementation of on-board refueling vapor recovery (ORVR) on new vehicles and make this as widespread as possible, which could reduce 97.5% of evaporative VOCs, as proved by Yang et al. (2015). Another more direct measure is to reduce the aromatic content in gasoline through optimizing oil refining techniques, which have a great effect on the organics composition of gasoline (Tang et al., 2015). For example, hydrofining techniques could significantly convert unsaturated hydrocarbons (i.e. alkenes and aromatics) to saturated alkanes. Unfortunately, the percentage of hydrofining technological processes employed is relatively lower in China (32.1%) compared with that in North America (53.2%) and Western Europe (49.2%) (Tang et al., 2015). Therefore, to improve the gasoline quality related to SOA formation in China, a direct measure to improve the percentage of hydrofining technological processes might be more acceptable and economical than implementing ORVR. Simultaneously, the aromatic content should be strictly considered in future gasoline evaluation systems, which is not only suitable for China, but also for those countries and regions in the world with extremely high aromatic content in gasoline.

Acknowledgements

This work was supported by the National Key R&D Program of China (2016YFC0202700), National Natural Science Foundation of China (41877306), Key Research Program of Frontier Sciences, CAS (QYZDB-SSW-DQC018) and Strategic Priority Research Program of the Chinese Academy of Sciences (XDB05010300).

Appendix A. Supplementary data

Supplementary data to this article can be found online at https://doi.org/10.1016/j.atmosenv.2019.01.001.

References

Ahlberg, E., Falk, J., Eriksson, A., Holst, T., Brune, W.H., Kristensson, A., Roldin, P., Svenningsson, B., 2017. Secondary organic aerosol from VOC mixtures in an oxidation flow reactor. Atmos. Environ. 161, 210–220. https://doi.org/10.1016/j.atmosenv.2017.05.005.

An, J., Wang, Y., Zhu, B., Wu, F., 2016. Measurements of O_3, NO_x and VOCs during summer in Beijing, China. Environ. Eng. Manag. J. 15, 715–724. https://doi.org/10.30638/eemj.2016.077.

Atkinson, R., Arey, J., 2003. Atmospheric degradation of volatile organic compounds. Chem. Rev. 103, 4605–4638. https://doi.org/10.1021/cr0206420.

Atkinson, R., Aschmann, S.M., Arey, J., Carter, W.P.L., 1989. Formation of ring-retaining products from the OH radical-initiated reactions of benzene and toluene. Int. J. Chem. Kinet. 21, 801–827. https://doi.org/10.1002/kin.550210907.

Bahreini, R., Middlebrook, A.M., de Gouw, J.A., Warneke, C., Trainer, M., Brock, C.A., Stark, H., Brown, S.S., Dube, W.P., Gilman, J.B., Hall, K., Holloway, J.S., Kuster, W.C., Perring, A.E., Prevot, A.S.H., Schwarz, J.P., Spackman, J.R., Szidat, S., Wagner, N.L., Weber, R.J., Zotter, P., Parrish, D.D., 2012. Gasoline emissions dominate over diesel in formation of secondary organic aerosol mass. Geophys. Res. Lett. 39, L06805. https://doi.org/10.1029/2011GL050718.

Baltaretu, C.O., Lichtman, E.I., Hadler, A.B., Elrod, M.J., 2009. Primary atmospheric oxidation mechanism for toluene. J. Phys. Chem. A 113, 221–230. https://doi.org/10.1021/jp806841t.

Bloss, C., Wagner, V., Bonzanini, A., Jenkin, M.E., Wirtz, K., Martin-Reviejo, M., Pilling, M.J., 2005a. Evaluation of detailed aromatic mechanisms (MCMv3 and MCMv3.1) against environmental chamber data. Atmos. Chem. Phys. 5, 623–639. https://doi.org/10.5194/acp-5-623-2005.

Bloss, C., Wagner, V., Jenkin, M.E., Volkamer, R., Bloss, W.J., Lee, J.D., Heard, D.E., Wirtz, K., Martin-Reviejo, M., Rea, G., Wenger, J.C., Pilling, M.J., 2005b. Development of a detailed chemical mechanism (MCMv3.1) for the atmospheric oxidation of aromatic hydrocarbons. Atmos. Chem. Phys. 5, 641–664. https://doi.org/10.5194/acp-5-641-2005.

Cai, C., Geng, F., Tie, X., Yu, Q., An, J., 2010. Characteristics and source apportionment of VOCs measured in Shanghai, China. Atmos. Environ. 44, 5005–5014. https://doi.org/10.1016/j.atmosenv.2010.07.059.

Chen, Q., Heald, C.L., Jimenez, J.L., Canagaratna, M.R., Zhang, Q., He, L.-Y., Huang, X.-F., Campuzano-Jost, P., Palm, B.B., Poulain, L., Kuwata, M., Martin, S.T., Abbatt, J.P.D., Lee, A.K.Y., Liggio, J., 2015. Elemental composition of organic aerosol: The gap between ambient and laboratory measurements. Geophys. Res. Lett. 42, 4182–4189. https://doi.org/10.1002/2015GL063693.

Chhabra, P.S., Flagan, R.C., Seinfeld, J.H., 2010. Elemental analysis of chamber organic aerosol using an aerodyne high-resolution aerosol mass spectrometer. Atmos. Chem. Phys. 10, 4111–4131. https://doi.org/10.5194/acp-10-4111-2010.

Chhabra, P.S., Ng, N.L., Canagaratna, M.R., Corrigan, A.L., Russell, L.M., Worsnop, D.R., Flagan, R.C., Seinfeld, J.H., 2011. Elemental composition and oxidation of chamber organic aerosol. Atmos. Chem. Phys. 11, 8827–8845. https://doi.org/10.5194/acp-11-8827-2011.

Choi, Y.-J., Ehrman, S.H., 2004. Investigation of sources of volatile organic carbon in the Baltimore area using highly time-resolved measurements. Atmos. Environ. 38, 775–791. https://doi.org/10.1016/j.atmosenv.2003.10.004.

Chu, B., Zhang, X., Liu, Y., He, H., Sun, Y., Jiang, J., Li, J., Hao, J., 2016. Synergetic formation of secondary inorganic and organic aerosol: effect of SO_2 and NH_3 on particle formation and growth. Atmos. Chem. Phys. 16, 14219–14230. https://doi.org/10.5194/acp-16-14219-2016.

Davidson, C.I., Phalen, R.F., Solomon, P.A., 2005. Airborne particulate matter and human health: a review. Aerosol Sci. Technol. 39, 737–749. https://doi.org/10.1080/02786820500191348.

de Gouw, J.A., Middlebrook, A.M., Warneke, C., Goldan, P.D., Kuster, W.C., Roberts, J.M., Fehsenfeld, F.C., Worsnop, D.R., Canagaratna, M.R., Pszenny, A.A.P., Keene, W.C., Marchewka, M., Bertman, S.B., Bates, T.S., 2005. Budget of organic carbon in a polluted atmosphere: Results from the New England Air Quality Study in 2002. J. Geophys. Res. Atmos. 110, D16305. https://doi.org/10.1029/2004JD005623.

Donahue, N.M., Robinson, A.L., Stanier, C.O., Pandis, S.N., 2006. Coupled partitioning,

dilution, and chemical aging of semivolatile organics. Environ. Sci. Technol. 40, 2635–2643. https://doi.org/10.1021/es052297c.
EIA, 2018. Energy Information Administration US: February 2018 Monthly Energy Review. DOE/EIA-0035(2018/2), available at: http://www.eia.gov/totalenergy/data/monthly/pdf/mer.pdf, Accessed date: 4 March 2018.
Farmer, D.K., Matsunaga, A., Docherty, K.S., Surratt, J.D., Seinfeld, J.H., Ziemann, P.J., Jimenez, J.L., 2010. Response of an aerosol mass spectrometer to organonitrates and organosulfates and implications for atmospheric chemistry. Proc. Natl. Acad. Sci. U.S.A. 107, 6670–6675. https://doi.org/10.1073/pnas.0912340107.
Forstner, H.J.L., Flagan, R.C., Seinfeld, J.H., 1997. Secondary organic aerosol from the photooxidation of aromatic hydrocarbons: molecular composition. Environ. Sci. Technol. 31, 1345–1358. https://doi.org/10.1021/es9605376.
Gentner, D.R., Isaacman, G., Worton, D.R., Chan, A.W.H., Dallmann, T.R., Davis, L., Liu, S., Day, D.A., Russell, L.M., Wilson, K.R., Weber, R., Guha, A., Harley, R.A., Goldstein, A.H., 2012. Elucidating secondary organic aerosol from diesel and gasoline vehicles through detailed characterization of organic carbon emissions. Proc. Natl. Acad. Sci. U.S.A. 109, 18318–18323. https://doi.org/10.1073/pnas.1212272109.
Gentner, D.R., Worton, D.R., Isaacman, G., Davis, L.C., Dallmann, T.R., Wood, E.C., Herndon, S.C., Goldstein, A.H., Harley, R.A., 2013. Chemical composition of gas-phase organic carbon emissions from motor vehicles and implications for ozone production. Environ. Sci. Technol. 47, 11837–11848. https://doi.org/10.1021/es401470e.
Gery, M.W., Fox, D.L., Jeffries, H.E., Stockburger, L., Weathers, W.S., 1985. A continuous stirred tank reactor investigation of the gas-phase reaction of hydroxyl radicals and toluene. Int. J. Chem. Kinet. 17, 931–955. https://doi.org/10.1002/kin.550170903.
Gordon, T.D., Presto, A.A., May, A.A., Nguyen, N.T., Lipsky, E.M., Donahue, N.M., Gutierrez, A., Zhang, M., Maddox, C., Rieger, P., Chattopadhyay, S., Maldonado, H., Maricq, M.M., Robinson, A.L., 2014. Secondary organic aerosol formation exceeds primary particulate matter emissions for light-duty gasoline vehicles. Atmos. Chem. Phys. 14, 4661–4678. https://doi.org/10.5194/acp-14-4661-2014.
Hallquist, M., Wenger, J.C., Baltensperger, U., Rudich, Y., Simpson, D., Claeys, M., Dommen, J., Donahue, N.M., George, C., Goldstein, A.H., Hamilton, J.F., Herrmann, H., Hoffmann, T., Iinuma, Y., Jang, M., Jenkin, M.E., Jimenez, J.L., Kiendler-Scharr, A., Maenhaut, W., McFiggans, G., Mentel, T.F., Monod, A., Prévôt, A.S.H., Seinfeld, J.H., Surratt, J.D., Szmigielski, R., Wildt, J., 2009. The formation, properties and impact of secondary organic aerosol: current and emerging issues. Atmos. Chem. Phys. 9, 5155–5236. https://doi.org/10.5194/acp-9-5155-2009.
Heald, C.L., Kroll, J.H., Jimenez, J.L., Docherty, K.S., DeCarlo, P.F., Aiken, A.C., Chen, Q., Martin, S.T., Farmer, D.K., Artaxo, P., 2010. A simplified description of the evolution of organic aerosol composition in the atmosphere. Geophys. Res. Lett. 37, L08803. https://doi.org/10.1029/2010GL042737.
Hildebrandt, L., Henry, K.M., Kroll, J.H., Worsnop, D.R., Pandis, S.N., Donahue, N.M., 2011. Evaluating the mixing of organic aerosol components using high-resolution aerosol mass spectrometry. Environ. Sci. Technol. 45, 6329–6335. https://doi.org/10.1021/es200825g.
Hu, W.W., Hu, M., Yuan, B., Jimenez, J.L., Tang, Q., Peng, J.F., Hu, W., Shao, M., Wang, M., Zeng, L.M., Wu, Y.S., Gong, Z.H., Huang, X.F., He, L.Y., 2013. Insights on organic aerosol aging and the influence of coal combustion at a regional receptor site of central eastern China. Atmos. Chem. Phys. 13, 10095–10112. https://doi.org/10.5194/acp-13-10095-2013.
Huang, R.-J., Zhang, Y., Bozzetti, C., Ho, K.-F., Cao, J.-J., Han, Y., Daellenbach, K.R., Slowik, J.G., Platt, S.M., Canonaco, F., Zotter, P., Wolf, R., Pieber, S.M., Bruns, E.A., Crippa, M., Ciarelli, G., Piazzalunga, A., Schwikowski, M., Abbaszade, G., Schnelle-Kreis, J., Zimmermann, R., An, Z., Szidat, S., Baltensperger, U., Haddad, I.E., Prevot, A.S.H., 2014. High secondary aerosol contribution to particulate pollution during haze events in China. Nature 514, 218–222. https://doi.org/10.1038/nature13774.
Jathar, S.H., Gordon, T.D., Hennigan, C.J., Pye, H.O.T., Pouliot, G., Adams, P.J., Donahue, N.M., Robinson, A.L., 2014. Unspeciated organic emissions from combustion sources and their influence on the secondary organic aerosol budget in the United States. Proc. Natl. Acad. Sci. U.S.A. 111, 10473–10478. https://doi.org/10.1073/pnas.1323740111.
Jathar, S.H., Miracolo, M.A., Tkacik, D.S., Donahue, N.M., Adams, P.J., Robinson, A.L., 2013. Secondary organic aerosol formation from photo-oxidation of unburned fuel: Experimental results and implications for aerosol formation from combustion emissions. Environ. Sci. Technol. 47, 12886–12893. https://doi.org/10.1021/es403445q.
Jenkin, M.E., Saunders, S.M., Wagner, V., Pilling, M.J., 2003. Protocol for the development of the Master Chemical Mechanism, MCM v3 (Part B): tropospheric degradation of aromatic volatile organic compounds. Atmos. Chem. Phys. 3, 181–193. https://doi.org/10.5194/acp-3-181-2003.
Ji, Y., Zhao, J., Terazono, H., Misawa, K., Levitt, N.P., Li, Y., Lin, Y., Peng, J., Wang, Y., Duan, L., Pan, B., Zhang, F., Feng, X., An, T., Marrero-Ortiz, W., Secrest, J., Zhang, A.L., Shibuya, K., Molina, M.J., Zhang, R., 2017. Reassessing the atmospheric oxidation mechanism of toluene. Proc. Natl. Acad. Sci. U.S.A. https://doi.org/10.1073/pnas.1705463114.
Jimenez, J.L., Canagaratna, M.R., Donahue, N.M., Prevot, A.S.H., Zhang, Q., Kroll, J.H., DeCarlo, P.F., Allan, J.D., Coe, H., Ng, N.L., Aiken, A.C., Docherty, K.S., Ulbrich, I.M., Grieshop, A.P., Robinson, A.L., Duplissy, J., Smith, J.D., Wilson, K.R., Lanz, V.A., Hueglin, C., Sun, Y.L., Tian, J., Laaksonen, A., Raatikainen, T., Rautiainen, J., Vaattovaara, P., Ehn, M., Kulmala, M., Tomlinson, J.M., Collins, D.R., Cubison, M.J., Dunlea, J., Huffman, J.A., Onasch, T.B., Alfarra, M.R., Williams, P.I., Bower, K., Kondo, Y., Schneider, J., Drewnick, F., Borrmann, S., Weimer, S., Demerjian, K., Salcedo, D., Cottrell, L., Griffin, R., Takami, A., Miyoshi, T., Hatakeyama, S., Shimono, A., Sun, J.Y., Zhang, Y.M., Dzepina, K., Kimmel, J.R., Sueper, D., Jayne, J.T., Herndon, S.C., Trimborn, A.M., Williams, L.R., Wood, E.C., Middlebrook, A.M., Kolb, C.E., Baltensperger, U., Worsnop, D.R., 2009. Evolution of organic aerosols in the atmosphere. Science 326, 1525–1529. https://doi.org/10.1126/science.1180353.
Karavalakis, G., Short, D., Vu, D., Russell, R., Hajbabaei, M., Asa-Awuku, A., Durbin, T.D., 2015. Evaluating the effects of aromatics content in gasoline on gaseous and particulate matter emissions from SI-PFI and SIDI vehicles. Environ. Sci. Technol. 49, 7021–7031. https://doi.org/10.1021/es5061726.
Klotz, B., Sørensen, S., Barnes, I., Becker, K.H., Etzkorn, T., Volkamer, R., Platt, U., Wirtz, K., Martín-Reviejo, M., 1998. Atmospheric oxidation of toluene in a large-volume outdoor photoreactor: in situ determination of ring-retaining product yields. J. Phys. Chem. A 102, 10289–10299. https://doi.org/10.1021/jp982719n.
Krechmer, J.E., Pagonis, D., Ziemann, P.J., Jimenez, J.L., 2016. Quantification of gas-wall partitioning in Teflon environmental chambers using rapid bursts of low-volatility oxidized species generated in situ. Environ. Sci. Technol. 50, 5757–5765. https://doi.org/10.1021/acs.est.6b00606.
Kroll, J.H., Chan, A.W.H., Ng, N.L., Flagan, R.C., Seinfeld, J.H., 2007. Reactions of semivolatile organics and their effects on secondary organic aerosol formation. Environ. Sci. Technol. 41, 3545–3550. https://doi.org/10.1021/es062059x.
Kroll, J.H., Ng, N.L., Murphy, S.M., Varutbangkul, V., Flagan, R.C., Seinfeld, J.H., 2005. Chamber studies of secondary organic aerosol growth by reactive uptake of simple carbonyl compounds. J. Geophys. Res. 110, D23207. https://doi.org/10.1029/2005jd006004.
Kroll, J.H., Seinfeld, J.H., 2008. Chemistry of secondary organic aerosol: Formation and evolution of low-volatility organics in the atmosphere. Atmos. Environ. 42, 3593–3624. https://doi.org/10.1016/j.atmosenv.2008.01.003.
Kulmala, M., 2003. How Particles Nucleate and Grow. Science 302, 1000–1001. https://doi.org/10.1126/science.1090848.
Kulmala, M., Vehkamäki, H., Petäjä, T., Dal Maso, M., Lauri, A., Kerminen, V.M., Birmili, W., McMurry, P.H., 2004. Formation and growth rates of ultrafine atmospheric particles: a review of observations. J. Aerosol Sci. 35, 143–176. https://doi.org/10.1016/j.jaerosci.2003.10.003.
Lambe, A.T., Onasch, T.B., Massoli, P., Croasdale, D.R., Wright, J.P., Ahern, A.T., Williams, L.R., Worsnop, D.R., Brune, W.H., Davidovits, P., 2011. Laboratory studies of the chemical composition and cloud condensation nuclei (CCN) activity of secondary organic aerosol (SOA) and oxidized primary organic aerosol (OPOA). Atmos. Chem. Phys. 11, 8913–8928. https://doi.org/10.5194/acp-11-8913-2011.
Li, L., Tang, P., Nakao, S., Chen, C.L., Cocker III, D.R., 2016a. Role of methyl group number on SOA formation from monocyclic aromatic hydrocarbons photooxidation under low-NO_x conditions. Atmos. Chem. Phys. 16, 2255–2272. https://doi.org/10.5194/acp-16-2255-2016.
Li, L., Tang, P., Nakao, S., Kacarab, M., Cocker, D.R., 2016b. Novel approach for evaluating secondary organic aerosol from aromatic hydrocarbons: Unified method for predicting aerosol composition and formation. Environ. Sci. Technol. 50, 6249–6256. https://doi.org/10.1021/acs.est.5b05778.
Liu, H., Man, H., Tschantz, M., Wu, Y., He, K., Hao, J., 2015a. VOC from vehicular evaporation emissions: Status and control strategy. Environ. Sci. Technol. 49, 14424–14431. https://doi.org/10.1021/acs.est.5b04064.
Liu, T., Wang, X., Deng, W., Hu, Q., Ding, X., Zhang, Y., He, Q., Zhang, Z., Lü, S., Bi, X., Chen, J., Yu, J., 2015b. Secondary organic aerosol formation from photochemical aging of light-duty gasoline vehicle exhausts in a smog chamber. Atmos. Chem. Phys. 15, 9049–9062. https://doi.org/10.5194/acp-15-9049-2015.
Liu, X.-H., Zhang, Y., Xing, J., Zhang, Q., Wang, K., Streets, D.G., Jang, C., Wang, W.-X., Hao, J.-M., 2010. Understanding of regional air pollution over China using CMAQ, part II. Process analysis and sensitivity of ozone and particulate matter to precursor emissions. Atmos. Environ. 44, 3719–3727. https://doi.org/10.1016/j.atmosenv.2010.03.036.
Liu, Y., Li, S.M., Liggio, J., 2014. Technical Note: application of positive matrix factor analysis in heterogeneous kinetics studies utilizing the mixed-phase relative rates technique. Atmos. Chem. Phys. 14, 9201–9211. https://doi.org/10.5194/acp-14-9201-2014.
Liu, Y., Shao, M., Lu, S., Chang, C.-C., Wang, J.-L., Fu, L., 2008. Source apportionment of ambient volatile organic compounds in the Pearl River Delta, China: Part II. Atmos. Environ. 42, 6261–6274. https://doi.org/10.1016/j.atmosenv.2008.02.027.
NBSC, 2017. National Bureau of Statistics of China: China Statistical Yearbook. China Statistics Press.
Ng, N.L., Canagaratna, M.R., Zhang, Q., Jimenez, J.L., Tian, J., Ulbrich, I.M., Kroll, J.H., Docherty, K.S., Chhabra, P.S., Bahreini, R., Murphy, S.M., Seinfeld, J.H., Hildebrandt, L., Donahue, N.M., DeCarlo, P.F., Lanz, V.A., Prévôt, A.S.H., Dinar, E., Rudich, Y., Worsnop, D.R., 2010. Organic aerosol components observed in northern hemispheric datasets from aerosol mass spectrometry. Atmos. Chem. Phys. 10, 4625–4641. https://doi.org/10.5194/acp-10-4625-2010.
Ng, N.L., Kroll, J.H., Chan, A.W.H., Chhabra, P.S., Flagan, R.C., Seinfeld, J.H., 2007. Secondary organic aerosol formation from m-xylene, toluene, and benzene. Atmos. Chem. Phys. 7, 3909–3922. https://doi.org/10.5194/acp-7-3909-2007.
Nordin, E.Z., Eriksson, A.C., Roldin, P., Nilsson, P.T., Carlsson, J.E., Kajos, M.K., Hellén, H., Wittbom, C., Rissler, J., Löndahl, J., Swietlicki, E., Svenningsson, B., Bohgard, M., Kulmala, M., Hallquist, M., Pagels, J.H., 2013. Secondary organic aerosol formation from idling gasoline passenger vehicle emissions investigated in a smog chamber. Atmos. Chem. Phys. 13, 6101–6116. https://doi.org/10.5194/acp-13-6101-2013.
Obermeyer, G., Aschmann, S.M., Atkinson, R., Arey, J., 2009. Carbonyl atmospheric reaction products of aromatic hydrocarbons in ambient air. Atmos. Environ. 43, 3736–3744. https://doi.org/10.1016/j.atmosenv.2009.04.015.
Odum, J.R., Hoffmann, T., Bowman, F., Collins, D., Flagan, R.C., Seinfeld, J.H., 1996. Gas/particle partitioning and secondary organic aerosol yields. Environ. Sci. Technol. 30, 2580–2585. https://doi.org/10.1021/es950943+.
Odum, J.R., Jungkamp, T.P.W., Griffin, R.J., Forstner, H.J.L., Flagan, R.C., Seinfeld, J.H., 1997. Aromatics, reformulated gasoline, and atmospheric organic aerosol formation. Environ. Sci. Technol. 31, 1890–1897. https://doi.org/10.1021/es9605351.
Pöschl, U., 2005. Atmospheric aerosols: composition, transformation, climate and health effects. Angew. Chem. Int. Ed. 44, 7520–7540. https://doi.org/10.1002/anie.200501122.
Paatero, P., 1997. Least squares formulation of robust non-negative factor analysis. Chemometr. Intell. Lab. Syst. 37, 23–35. https://doi.org/10.1016/S0169-7439(96)00044-5.
Paatero, P., Tapper, U., 1994. Positive matrix factorization: a non-negative factor model with optimal utilization of error estimates of data values. Environmetrics 5, 111–126. https://doi.org/10.1002/env.3170050203.

Pankow, J.F., 1994. An absorption model of the gas/aerosol partitioning involved in the formation of secondary organic aerosol. Atmos. Environ. 28, 189–193. https://doi.org/10.1016/1352-2310(94)90094-9.
Peng, J., Hu, M., Du, Z., Wang, Y., Zheng, J., Zhang, W., Yang, Y., Qin, Y., Zheng, R., Xiao, Y., Wu, Y., Lu, S., Wu, Z., Guo, S., Mao, H., Shuai, S., 2017. Gasoline aromatics: a critical determinant of urban secondary organic aerosol formation. Atmos. Chem. Phys. 17, 10743–10752. https://doi.org/10.5194/acp-17-10743-2017.
Peng, J., Hu, M., Gong, Z., Tian, X., Wang, M., Zheng, J., Guo, Q., Cao, W., Lv, W., Hu, W., Wu, Z., Guo, S., 2016. Evolution of secondary inorganic and organic aerosols during transport: A case study at a regional receptor site. Environ. Pollut. 218, 794–803. https://doi.org/10.1016/j.envpol.2016.08.003.
Platt, S.M., El Haddad, I., Zardini, A.A., Clairotte, M., Astorga, C., Wolf, R., Slowik, J.G., Temime-Roussel, B., Marchand, N., Ježek, I., Drinovec, L., Močnik, G., Möhler, O., Richter, R., Barmet, P., Bianchi, F., Baltensperger, U., Prévôt, A.S.H., 2013. Secondary organic aerosol formation from gasoline vehicle emissions in a new mobile environmental reaction chamber. Atmos. Chem. Phys. 13, 9141–9158. https://doi.org/10.5194/acp-13-9141-2013.
Platt, S.M., Haddad, I.E., Pieber, S.M., Huang, R.J., Zardini, A.A., Clairotte, M., Suarez-Bertoa, R., Barmet, P., Pfaffenberger, L., Wolf, R., Slowik, J.G., Fuller, S.J., Kalberer, M., Chirico, R., Dommen, J., Astorga, C., Zimmermann, R., Marchand, N., Hellebust, S., Temime-Roussel, B., Baltensperger, U., Prévôt, A.S.H., 2014. Two-stroke scooters are a dominant source of air pollution in many cities. Nat. Commun. 5, 3749. https://doi.org/10.1038/ncomms4749.
Robinson, A.L., Donahue, N.M., Shrivastava, M.K., Weitkamp, E.A., Sage, A.M., Grieshop, A.P., Lane, T.E., Pierce, J.R., Pandis, S.N., 2007. Rethinking organic aerosols: semi-volatile emissions and photochemical aging. Science 315, 1259–1262. https://doi.org/10.1126/science.1133061.
Rollins, A.W., Kiendler-Scharr, A., Fry, J.L., Brauers, T., Brown, S.S., Dorn, H.P., Dube, W.P., Fuchs, H., Mensah, A., Mentel, T.F., Rohrer, F., Tillmann, R., Wegener, R., Wooldridge, P.J., Cohen, R.C., 2009. Isoprene oxidation by nitrate radical: Alkyl nitrate and secondary organic aerosol yields. Atmos. Chem. Phys. 9, 6685–6703. https://doi.org/10.5194/acp-9-6685-2009.
Saleh, R., Donahue, N.M., Robinson, A.L., 2013. Time scales for gas-particle partitioning equilibration of secondary organic aerosol formed from alpha-pinene ozonolysis. Environ. Sci. Technol. 47, 5588–5594. https://doi.org/10.1021/es400078d.
Sato, K., Takami, A., Isozaki, T., Hikida, T., Shimono, A., Imamura, T., 2010. Mass spectrometric study of secondary organic aerosol formed from the photo-oxidation of aromatic hydrocarbons. Atmos. Environ. 44, 1080–1087. https://doi.org/10.1016/j.atmosenv.2009.12.013.
Sato, K., Takami, A., Kato, Y., Seta, T., Fujitani, Y., Hikida, T., Shimono, A., Imamura, T., 2012. AMS and LC/MS analyses of SOA from the photooxidation of benzene and 1,3,5-trimethylbenzene in the presence of NOx: effects of chemical structure on SOA aging. Atmos. Chem. Phys. 12, 4667–4682. https://doi.org/10.5194/acp-12-4667-2012.
Seuwen, R., Warneck, P., 1996. Oxidation of toluene in NO_x free air: Product distribution and mechanism. Int. J. Chem. Kinet. 28, 315–332. https://doi.org/10.1002/%28sici%291097-4601%281996%2928:5%3c315::aid-kin1%3e3.0.co;2-y.
Smith, D.F., McIver, C.D., Kleindienst, T.E., 1998. Primary product distribution from the reaction of hydroxyl radicals with toluene at ppb NO_x mixing ratios. J. Atmos. Chem. 30, 209–228. https://doi.org/10.1023/a:1005980301720.
Song, Y., Shao, M., Liu, Y., Lu, S., Kuster, W., Goldan, P., Xie, S., 2007. Source apportionment of ambient volatile organic compounds in Beijing. Environ. Sci. Technol. 41, 4348–4353. https://doi.org/10.1021/es0625982.
Takekawa, H., Minoura, H., Yamazaki, S., 2003. Temperature dependence of secondary organic aerosol formation by photo-oxidation of hydrocarbons. Atmos. Environ. 37, 3413–3424. https://doi.org/10.1016/s1352-2310(03)00359-5.
Tang, G., Sun, J., Wu, F., Sun, Y., Zhu, X., Geng, Y., Wang, Y., 2015. Organic composition of gasoline and its potential effects on air pollution in North China. Sci. China Chem. 58, 1416–1425. https://doi.org/10.1007/s11426-015-5464-0.
Thalman, R., de Sá, S.S., Palm, B.B., Barbosa, H.M.J., Pöhlker, M.L., Alexander, M.L., Brito, J., Carbone, S., Castillo, P., Day, D.A., Kuang, C., Manzi, A., Ng, N.L., Sedlacek Iii, A.J., Souza, R., Springston, S., Watson, T., Pöhlker, C., Pöschl, U., Andreae, M.O., Artaxo, P., Jimenez, J.L., Martin, S.T., Wang, J., 2017. CCN activity and organic hygroscopicity of aerosols downwind of an urban region in central Amazonia: seasonal and diel variations and impact of anthropogenic emissions. Atmos. Chem. Phys. 17, 11779–11801. https://doi.org/10.5194/acp-17-11779-2017.
Tröstl, J., Chuang, W.K., Gordon, H., Heinritzi, M., Yan, C., Molteni, U., Ahlm, L., Frege, C., Bianchi, F., Wagner, R., Simon, M., Lehtipalo, K., Williamson, C., Craven, J.S., Duplissy, J., Adamov, A., Almeida, J., Bernhammer, A.-K., Breitenlechner, M., Brilke, S., Dias, A., Ehrhart, S., Flagan, R.C., Franchin, A., Fuchs, C., Guida, R., Gysel, M., Hansel, A., Hoyle, C.R., Jokinen, T., Junninen, H., Kangasluoma, J., Keskinen, H., Kim, J., Krapf, M., Kürten, A., Laaksonen, A., Lawler, M., Leiminger, M., Mathot, S., Möhler, O., Nieminen, T., Onnela, A., Petäjä, T., Piel, F.M., Miettinen, P., Rissanen, M.P., Rondo, L., Sarnela, N., Schobesberger, S., Sengupta, K., Sipilä, M., Smith, J.N., Steiner, G., Tomè, A., Virtanen, A., Wagner, A.C., Weingartner, E., Wimmer, D., Winkler, P.M., Ye, P., Carslaw, K.S., Curtius, J., Dommen, J., Kirkby, J., Kulmala, M., Riipinen, I., Worsnop, D.R., Donahue, N.M., Baltensperger, U., 2016. The role of low-volatility organic compounds in initial particle growth in the atmosphere. Nature 533, 527–531. https://doi.org/10.1038/nature18271.
Trump, E.R., Riipinen, I., Donahue, N.M., 2014. Interactions between atmospheric ultrafine particles and secondary organic aerosol mass: a model study. Boreal Environ. Res. 19, 352–362. http://hdl.handle.net/10138/228623.
Ulbrich, I.M., Canagaratna, M.R., Zhang, Q., Worsnop, D.R., Jimenez, J.L., 2009. Interpretation of organic components from positive matrix factorization of aerosol mass spectrometric data. Atmos. Chem. Phys. 9, 2891–2918. https://doi.org/10.5194/acp-9-2891-2009.
Van der Westhuisen, H., Taylor, A.B., Bell, A.J., Mbarawa, M., 2004. Evaluation of evaporative emissions from gasoline powered motor vehicles under South African conditions. Atmos. Environ. 38, 2909–2916. https://doi.org/10.1016/j.atmosenv.2004.02.024.
Volkamer, R., Klotz, B., Barnes, I., Imamura, T., Wirtz, K., Washida, N., Becker, K.H., Platt, U., 2002. OH-initiated oxidation of benzene Part I. Phenol formation under atmospheric conditions. Phys. Chem. Chem. Phys. 4, 1598–1610. https://doi.org/10.1039/B108747A.
Volkamer, R., Platt, U., Wirtz, K., 2001. Primary and secondary glyoxal formation from aromatics: experimental evidence for the bicycloalkyl−radical pathway from benzene, toluene, and p-xylene. J. Phys. Chem. A 105, 7865–7874. https://doi.org/10.1021/jp010152w.
Wang, Y., Zheng, R., Qin, Y., Peng, J., Li, M., Lei, J., Wu, Y., Hu, M., Shuai, S., 2016. The impact of fuel compositions on the particulate emissions of direct injection gasoline engine. Fuel 166, 543–552. https://doi.org/10.1016/j.fuel.2015.11.019.
Wang, Z., Wu, Z., Yue, D., Shang, D., Guo, S., Sun, J., Ding, A., Wang, L., Jiang, J., Guo, H., Gao, J., Cheung, H.C., Morawska, L., Keywood, M., Hu, M., 2017. New particle formation in China: Current knowledge and further directions. Sci. Total Environ. 577, 258–266. https://doi.org/10.1016/j.scitotenv.2016.10.177.
Watson, J.G., Chow, J.C., Fujita, E.M., 2001. Review of volatile organic compound source apportionment by chemical mass balance. Atmos. Environ. 35, 1567–1584. https://doi.org/10.1016/S1352-2310(00)00461-1.
Wu, R., Li, J., Hao, Y., Li, Y., Zeng, L., Xie, S., 2016. Evolution process and sources of ambient volatile organic compounds during a severe haze event in Beijing, China. Sci. Total Environ. 560, 62–72. https://doi.org/10.1016/j.scitotenv.2016.04.030.
Wu, R., Pan, S., Li, Y., Wang, L., 2014. Atmospheric oxidation mechanism of toluene. J. Phys. Chem. A 118, 4533–4547. https://doi.org/10.1021/jp500077f.
Yamada, H., 2013. Contribution of evaporative emissions from gasoline vehicles toward total VOC emissions in Japan. Sci. Total Environ. 449, 143–149. https://doi.org/10.1016/j.scitotenv.2013.01.045.
Yan, C., Nie, W., Äijälä, M., Rissanen, M.P., Canagaratna, M.R., Massoli, P., Junninen, H., Jokinen, T., Sarnela, N., Häme, S.A.K., Schobesberger, S., Canonaco, F., Yao, L., Prévôt, A.S.H., Petäjä, T., Kulmala, M., Sipilä, M., Worsnop, D.R., Ehn, M., 2016. Source characterization of highly oxidized multifunctional compounds in a boreal forest environment using positive matrix factorization. Atmos. Chem. Phys. 16, 12715–12731. https://doi.org/10.5194/acp-16-12715-2016.
Yang, X., Liu, H., Cui, H., Man, H., Fu, M., Hao, J., He, K., 2015. Vehicular volatile organic compounds losses due to refueling and diurnal process in China: 2010–2050. J. Environ. Sci. 33, 88–96. https://doi.org/10.1016/j.jes.2015.01.012.
Ye, P., Ding, X., Hakala, J., Hofbauer, V., Robinson, E.S., Donahue, N.M., 2016. Vapor wall loss of semi-volatile organic compounds in a Teflon chamber. Aerosol Sci. Technol. 50, 822–834. https://doi.org/10.1080/02786826.2016.1195905.
Zervas, E., Montagne, X., Lahaye, J., 1999. The influence of gasoline formulation on specific pollutant emissions. J. Air Waste Manage. 49, 1304–1314. https://doi.org/10.1080/10473289.1999.10463969.
Zhang, R., Wang, G., Guo, S., Zamora, M.L., Ying, Q., Lin, Y., Wang, W., Hu, M., Wang, Y., 2015a. Formation of urban fine particulate matter. Chem. Rev. 115, 3803–3855. https://doi.org/10.1021/acs.chemrev.5b00067.
Zhang, X., Cappa, C.D., Jathar, S.H., McVay, R.C., Ensberg, J.J., Kleeman, M.J., Seinfeld, J.H., 2014. Influence of vapor wall loss in laboratory chambers on yields of secondary organic aerosol. Proc. Natl. Acad. Sci. U.S.A. 111, 5802–5807. https://doi.org/10.1073/pnas.1404727111.
Zhang, X., Schwantes, R.H., McVay, R.C., Lignell, H., Coggon, M.M., Flagan, R.C., Seinfeld, J.H., 2015b. Vapor wall deposition in Teflon chambers. Atmos. Chem. Phys. 15, 4197–4214. https://doi.org/10.5194/acp-15-4197-2015.
Zhao, Y., Hennigan, C.J., May, A.A., Tkacik, D.S., de Gouw, J.A., Gilman, J.B., Kuster, W.C., Borbon, A., Robinson, A.L., 2014. Intermediate-volatility organic compounds: a large source of secondary organic aerosol. Environ. Sci. Technol. 48, 13743–13750. https://doi.org/10.1021/es5035188.
Zhao, Y., Nguyen, N.T., Presto, A.A., Hennigan, C.J., May, A.A., Robinson, A.L., 2015. Intermediate volatility organic compound emissions from on-road diesel vehicles: Chemical composition, emission factors, and estimated secondary organic aerosol production. Environ. Sci. Technol. 49, 11516–11526. https://doi.org/10.1021/acs.est.5b02841.
Zhao, Y., Nguyen, N.T., Presto, A.A., Hennigan, C.J., May, A.A., Robinson, A.L., 2016. Intermediate volatility organic compound Emissions from on-road gasoline vehicles and small off-road gasoline engines. Environ. Sci. Technol. 50, 4554–4563. https://doi.org/10.1021/acs.est.5b06247.
Zhao, Y., Saleh, R., Saliba, G., Presto, A.A., Gordon, T.D., Drozd, G.T., Goldstein, A.H., Donahue, N.M., Robinson, A.L., 2017. Reducing secondary organic aerosol formation from gasoline vehicle exhaust. Proc. Natl. Acad. Sci. U.S.A. 114, 6984–6989. https://doi.org/10.1073/pnas.1620911114.
Zhou, Y., Zhang, H., Parikh, H.M., Chen, E.H., Rattanavaraha, W., Rosen, E.P., Wang, W., Kamens, R.M., 2011. Secondary organic aerosol formation from xylenes and mixtures of toluene and xylenes in an atmospheric urban hydrocarbon mixture: Water and particle seed effects (II). Atmos. Environ. 45, 3882–3890. https://doi.org/10.1016/j.atmosenv.2010.12.048.
Zou, Y., Deng, X.J., Zhu, D., Gong, D.C., Wang, H., Li, F., Tan, H.B., Deng, T., Mai, B.R., Liu, X.T., Wang, B.G., 2015. Characteristics of 1 year of observational data of VOCs, NO_x and O_3 at a suburban site in Guangzhou, China. Atmos. Chem. Phys. 15, 6625–6636. https://doi.org/10.5194/acp-15-6625-2015.